

1  
2 **The Significance of Seismic Wavespeed Minima and Thermal Maxima in the**  
3 **Mantle and the Role of Dynamic Melting**

4  
5 **Don L. Anderson<sup>a</sup> and Charles G. Sammis<sup>b</sup>**  
6

7 <sup>a</sup>Seismological Laboratory, California Institute of Technology, Pasadena, CA  
8 91125, USA

9 <sup>b</sup>Department of Earth Sciences, University of Southern California, Los Angeles,  
10 CA 90089-0740, USA

11  
12 Short title: Wavespeed Minima in Earth's Mantle

13  
14 Key Words: intra-plate volcanism, seismic low-velocity zone, mantle plumes.  
15

**16 Abstract**

17

18 It is widely assumed that the boundary layer above the core is the source of intraplate volcanoes  
19 such as Hawaii, Samoa and Yellowstone and that the sub-plate boundary layer at the top of the  
20 mantle is thin and entirely subsolidus. In fact, this layer is thicker and has higher expansivity,  
21 buoyancy and insulating power than the lower one, and may have higher potential temperatures. The  
22 observed seismic structure of the low-velocity zone (LVZ) including attenuation, anisotropy, sharp  
23 boundaries and a reduction of both compressional and shear moduli can be taken as strong evidence  
24 for the ubiquitous presence of melt in the upper mantle. If the LVZ contains as little as 1-2% melt  
25 then it is the most plausible and accessible source for mid-plate magmas; deeply rooted active  
26 upwellings are unnecessary. The upper boundary layer is also the most plausible source of ancient  
27 isotopic signatures of these magmas and their inclusions.

28

## 29 Introduction

30 Seismological arguments for a melt component in the upper mantle extend back nearly 50 years (1-  
31 3). It was realized that, while normal P-T gradients in the mantle cause a minimum of seismic  
32 wavespeeds at depths between about 100 and 200 km, the actual properties of this region require  
33 something more. By 1970 geophysicists had shown that the missing ingredient is probably athermal,  
34 such as stress- and volatile-enhanced melting (1-6). Low velocity zones in the mantle are now routinely  
35 attributed to dehydration melting although CO<sub>2</sub> and dynamic melting may play important roles. The  
36 theory for the interaction of elastic waves with partially molten rock was well developed prior to 1970  
37 (1, 5, 7), and provides a self-consistent explanation of reduced seismic velocities, increased anisotropy,  
38 and high attenuation of seismic waves in the low velocity zone. An elastic wave can be viewed as a time  
39 dependent stress and temperature perturbation to the thermodynamic state of the medium (1, 7, 8). In  
40 regions near the melting point it can promote a small amount of crystallization or melting. The  
41 associated volume change introduces a strain in the medium, which lowers the ratio of stress to strain  
42 resulting in a reduced seismic velocity. This magnifies the effect of a small amount of melt on  
43 wavespeeds beyond that given by simple static volume averaging (1, 5, 9).

44 The precipitous change in elastic velocities at the onset of partial melting explains the sharp  
45 variable-depth boundaries of the LVZ, the G and the L discontinuities. The global G discontinuity at the  
46 top of the LVZ is an abrupt 7-8% reduction in short-period shear-wave speeds, which has been attributed  
47 to sub-horizontal melt-rich lamellae (10). Comparable drops are inferred for compressional waves. The  
48 existence of converted phases from the lid-LVZ interface provides evidence that the interface is sharp,  
49 not diffuse as is expected at the lithosphere-asthenosphere boundary, which represents the transition  
50 from long-term strength to weakness on geological time scales. Waveform modeling indicates seismic  
51 velocity drops of up to 10–20% (11). Beneath the central Pacific, shear wave reverberations imply  
52 abrupt 5-14 % velocity drops at depths that vary from 66 to 80 km (12), and a further 8–9% gradual  
53 decrease from the top of the LVZ to about 160 km (13,14). Below continental shields, the upper  
54 boundary of the LVZ is depressed to 150 km.

55 If G and L represent boundaries of the partial melt zone (9, 12-14), the implication is that volatiles  
56 have drained upwards and the melt content decreases with depth below the axis of the LVZ (Fig. 1).  
57 Melts can be shear-driven and compaction-driven as well as buoyancy-driven. In other words, volcanoes  
58 can be, and probably are, the result of stresses and fractures associated with plate tectonics rather than  
59 localized 'hotspots'. This tectonic paradigm has been challenged recently by arguments that melts do not

60 occur in the LVZ, that they drain out quickly, or that the effect is too small to explain the seismic  
61 observations (15-17). These arguments ignore the importance of interactions of stress waves with small  
62 melt fractions (5, 18) in the transmitting media, interactions of migrating melts with the matrix and the  
63 role of impermeable interfaces.

64 The competing paradigm is that only mantle plumes are hot enough to produce melt and to have  
65 sufficiently deep roots to supply magmas with ancient-enriched and “undegassed” mantle isotope  
66 signatures. These geochemical inferences are based on implausible assumptions about ambient mantle,  
67 the geotherm, the mode of mantle convection, and the nature and physical state of the surface boundary  
68 layer (19), which is usually ignored.

69

### 70 **Analog experiments**

71 The response of a partially molten solid to the transmission of elastic waves is different from that of  
72 a fluid-saturated but unreactive porous solid (1, 8). Several studies have determined the variation of  
73 elastic wave velocities across the melting point (1, 17, 18-23) (Fig. 2). Note the abrupt drops in  
74 wavespeeds at the eutectic temperature. Similar effects may explain the G - or Gutenberg discontinuity,  
75 and other LVZs associated with phase changes in the deeper mantle, but a solid-melt interface is not  
76 required ) (7, 8). Additional details on relevant analog experiments and a discussion of deep LVZs are in  
77 the Appendix.

78

### 79 **Geochemistry**

80 The upper boundary layer of the mantle is composed primarily (>97%) of refractory high-melting  
81 lithologies, e.g. dunite or harzburgite, that collect at the top of the mantle because they are buoyant and  
82 which may trap fragments of ancient mantle, including high  $^3\text{He}/^4\text{He}$  gases or low-U,Th inclusions (9,  
83 24, 25). The interleaved low rigidity layers probably account for 1-2 % of the volume, and may be  
84 pyroxenite, magma-mush lenses, sills, metasomatic lamellae or fine-grained shear zones, which are  
85 large-scale versions of the veins in metasomatized ‘lithosphere’. Trace “exotic” components, such as  
86 sulfides, oxides, carbonatites and fluid inclusions collect in the surface layers because of their solubility,  
87 density, mobility and volatility and appear to resolve the various U-Pb-He-heatflow, ocean island basalt  
88 and delayed core-formation paradoxes (19, 24, 26-28). Although the highest potential temperatures in  
89 the mantle are likely to coincide with the LVZ (24, 29), low-melting fertile lithologies such as dense  
90 eclogites and pyroxenites collect at the base of the transition zone. The potential temperature of any

91 volume in the mantle is the temperature that that volume would have if it were compressed or expanded  
92 to some reference pressure. It is often erroneously assumed in the petrological literature that this is the  
93 extension of an actual sub-plate adiabatic geotherm.

94 The canonical models of mantle geochemistry and petrology assume that, except under ridges  
95 (melting due to decompression melting), trenches (melting due to water induced melting) and hotspots  
96 (melting due to anomalous temperature), the upper mantle is entirely subsolidus (5, 30, 31) and that the  
97 boundary layer above the core is the most plausible source of intraplate volcanoes such as Hawaii,  
98 Samoa and Yellowstone (30, 32-34). The so-called basal mélange is assumed to be the largest, hottest,  
99 most accessible, least degassed and most “primordial” (defined as having  $^3\text{He}/^4\text{He}$  ratios higher than an  
100 average mid-ocean-range basalt MORB) part of the mantle. From classical physics and logical points of  
101 view (19) these assumptions are based on a number of questionable premises: 1) upper mantle geotherms  
102 cannot cross the solidi of mantle minerals, and cannot exceed  $\sim 1400^\circ\text{C}$  or temperatures assigned to sub-  
103 ridge mantle (31, 35-38), 2) high  $^3\text{He}/^4\text{He}$  ratios in mid-plate magmas relative to those in average MORB  
104 are due to excess  $^3\text{He}$  (not low  $^4\text{He}$ ), and 3) most of the mantle supports an adiabatic gradient and is not  
105 cooling with time. However, geotherms depend on thermal history and on the distribution of radioactive  
106 elements. Internal heating, and by inference, secular cooling modulated by internal heating, lead to a  
107 temperature maximum in the shallow mantle, and a subadiabatic gradient throughout most of the mantle  
108 (29, 39-41). This thermal max results in an inverted geotherm, or overshoot, which probably coincides  
109 with the LVZ (Fig. 1). The base of the surface boundary layer and the base of the mantle cannot be  
110 assumed to be non-cooling isotherms (31, 41).

111 | High  $^3\text{He}/^4\text{He}$  ratios in mid-plate magmas relative to those in average MORB cannot be taken as  
112 evidence that they have a deep origin (9, 24, 26). Basalt isotope chemistry is controlled by mixing of  
113 components (26), but both mixing relations and isotope evolution trajectories are indifferent as to the  
114 location, depth, size and absolute compositions of the components. This means that the mixture of a high  
115  $^3\text{He}/^4\text{He}$ -low  $^3\text{He}$  component, long resident in the shallow mantle, and a high  $^3\text{He}$ -low  $^3\text{He}/^4\text{He}$   
116 component such as MORB is indistinguishable from the signatures attributed to deep undegassed or  
117 primordial mantle sources.

118

### 119 **The Geotherm**

120 Curve fitting assumptions, adjustments of the data, anelastic corrections, experimental errors and  
121 theoretical oversights have led to the view that ambient midplate upper mantle is colder and less variable

l22 than a straightforward analysis of bathymetric and seismic data would indicate (18-21). Cambridge  
l23 geotherms, for example, are required to converge at depth, and to be asymptotic to the MORB adiabat  
l24 (31, 35). In other words, temperatures are forced to bend as they approach 1400 °C or an a priori adiabat.  
l25 Such constrained temperatures are more than 300 °C lower than would be inferred from the same data  
l26 without this enforced bend (36, 37). This has led to the view that temperatures that are higher than the  
l27 constrained adiabats are anomalous and require deep mantle sources.

l28 Both vertical and lateral temperature gradients are high in conduction boundary layers. Basalts  
l29 derived from 150 km depth in a mature boundary layer will, in general, be hotter than those derived from  
l30 60 km depth but may involve lower extents of melting (42). A given isotherm deepens with time. There  
l31 are several lines of evidence that sub-boundary layer temperatures, however, increase away from ridges  
l32 toward plate interiors. The central Pacific has much lower upper mantle wavespeeds and higher inferred  
l33 temperatures than other oceans and than global reference models (43). Near-ridge mantle below 200 km  
l34 depth has higher shear velocities, on average, than midplate upper mantle (24, 43, 44). Bathymetry data  
l35 yields mantle temperatures for ‘normal’ regions of the north Pacific that are ~200°C higher than the  
l36 constrained temperatures (16, 31, 38, 45). Subsidence rates and residual bathymetry of the younger  
l37 portions of plates imply that sub-ridge mantle is denser, on average, and in the southern oceans, than  
l38 mantle under older plates. Geophysical data are consistent with petrological inferences that near-ridge  
l39 mantle and midplate mantle temperatures differ, on average, by >100°C but also show that the higher  
l40 temperatures are widespread and reflect ambient mantle under plates while lower temperatures appear to  
l41 preferentially occur under young oceanic plates or to be sampled by midplate volcanoes that extract  
l42 magma from the upper parts of the boundary layer. Hawaii, therefore, is not a localized thermal anomaly  
l43 associated with a plume; it is a small-scale sample of a deep portion of ambient midplate boundary layer  
l44 mantle (24, 46, 47). Its location and magma output are controlled by a step in the thickness of the plate at  
l45 the wide Molokai fracture zone (48), and by stresses in the plate, not by conditions at the core-mantle  
l46 boundary.

l47 | The maximum depth of melting, and inferred source temperature, of oceanic magmas increases, and  
l48 the fraction of melt decreases, with plate age (42, 46). The P-T-depth-age trajectories calculated for  
l49 midplate magmas track the 1500-1600°C cooling half-space isotherms, rather than the predicted 1300°C  
l50 horizontal isotherm (24, 45). Petrological and seismic data are consistent with midplate magmas being  
l51 extracted from within and near the base of the boundary layer, which has maximum temperatures some  
l52 ~200°C higher than generally assumed for ambient mantle. On the other hand the low temperatures, low

153 diffusivity, and high strength and buoyancy of the outer part of the shell mean the upper boundary layer  
154 is also the most plausible place to preserve ancient enriched, isotopic signatures. These considerations  
155 turn canonical geochemical models on their heads (30, 32-34, 49) and remove what have been  
156 considered as geochemical paradoxes and inconsistencies between geochemical and geophysical models.  
157

## 158 **Discussion**

159 It is significant that the magnitude of the anisotropy in the LVZ is about the same as the drop in  
160 wavespeed at the lid-LVZ boundary (the G-discontinuity). This supports the sheared multiphase  
161 aggregate model with low-rigidity oriented lamellae (10, 24, 50). In such a model, melt segregates into  
162 sub-horizontal layers that lubricate plate motion. This interpretation is further supported by observations  
163 of strong heterogeneity above 200 km depth and the numerous reflections, both S- wave and P-wave  
164 between 100 and 200 km depth. The number of reflections in this depth range exceeds the number  
165 observed near 400 km depth (51). Variations in  $V_p$  of 7.8%, in  $V_s$  of 14.5% and in  $V_p/V_s$  of 7.2%  
166 correspond to very high temperature variations, 850 to 960 K, or small amounts of melt.

167 Anisotropy and strong reflections at the boundaries of the LVZ are best explained by large lenses of  
168 aligned/segregated melt accumulations [LLAMA] (9, 10, 24, 50). The interface (the G-discontinuity)  
169 and the L-discontinuity correspond to solidi, solidification or zone-refined fronts or volatile-no-volatile  
170 boundaries. Others have equated the much thinner mechanical boundary layer and the lithosphere to the  
171 lid (16) and sought to explain rheological transitions in terms of water content, grain size or  
172 thermal/compositional effects (36, 52, 53). The sharp boundaries, anisotropy and bulk modulus of the  
173 LVZ cannot be explained with these effects or with simple static volume averaging schemes.

174 Melt-rich layers in a sheared mélange are tilted relative to the shear plane (54) This explains shear-  
175 wave splitting and the apparent tilts of low wavespeed features in the mantle. It has been argued that that  
176 gravity will effectively drain out all the melt along these tilted interfaces and that gravity-driven fluid  
177 dynamic instabilities will destroy any such layers that survive (15). However, the melt channels are  
178 probably not continuous, they react with the matrix and they are constantly reforming in the shear field.

179 Volume changing solid-solid and liquid-solid phase transformations can be effective in lowering  
180 elastic moduli (7, 55). Even if such volume changes are small, their effect on the stress-strain relation  
181 can be large. The main question is, can a high frequency seismic wave change the thermodynamic state  
182 fast enough so that volume changes occur in the medium? Since the effect is measured at laboratory

183 frequencies (1, 21), the answer is probably yes. The fact that the absorption band overlaps the seismic  
184 band (9) supports this conclusion.

185 If melt is concentrated in thin lamellae, only about 1-2 vol. % is required to account for the  
186 amplitudes of the observed reflections and anisotropy (9, 10, 24). This is greater than the static  
187 equilibrium melt fraction at the mantle temperatures and compositions that are assumed in petrological  
188 models (16). However, the BL may be hotter or of different composition than in the experiments (6, 19,  
189 46). The melt fraction in LLAMA may also be enhanced by accumulation of melts that have migrated or  
190 been sheared in from greater depths or zone-refined in from above.

191 High-resolution seismic imaging (10, 56-59) and rock physics experiments (50, 54), give strong  
192 support to the type of model discussed here. A heterogeneous sheared boundary layer source model not  
193 only explains a variety of geophysical data but has provided evidence that midplate volcanoes are often  
194 underlain by higher wavespeeds at shallow depths than occur under ridges and some volcano-free areas  
195 (43, 44, 57), suggesting that melt extraction may have created high wavespeed areas. Large offsets  
196 between deep low wavespeed mantle features and volcanoes are commonly observed suggesting that  
197 they may be unrelated.

198

## 199 **Summary**

200 The causes of low velocities, high attenuation and anisotropy in the Earth's upper mantle have  
201 recently become controversial. The plate tectonic paradigm for intraplate volcanism, which involves  
202 stress release of indigenous melts in the LVZ, has been challenged with arguments that assert that  
203 melts do not occur in the LVZ or that if they do they drain out quickly or that even if they don't  
204 drain out the effect is too small to explain the seismic observations (15-17). The theory used,  
205 however, does not explain the laboratory data on partially molten materials that motivated the idea in  
206 the first place (1, 21). This apparent paradox is due to the neglect of the pertinent physics. Models  
207 that claim to rule out upper mantle melts assume that a melt phase is an unreactive component that  
208 can be accounted for by volume averaging and conclude that small amounts of melt do not have a  
209 large effect on seismic velocities (15, 16). These studies ignore experiments and theory that show the  
210 ability of small amounts of melt to dramatically modify physical properties, including permeability,  
211 through chemical effects (7, 8). The interaction between seismic waves and melt, and of migrating  
212 melts with the matrix, are significant. The effects of fluids are also not entirely microscopic; the  
213 presence of large lamellae and sills are consistent with observed seismic anisotropy in the LVZ (10,



214 24).

215 Taken as a whole, the seismic structure of the LVZ, including attenuation, sharp boundaries, and  
216 anisotropy are best explained using a dynamic melting model. The implication is that the LVZ  
217 contains melt and that it is not only a plausible source, but it is the most likely source for mid-plate  
218 and large igneous province volcanism (4, 60, 61). Sources deeper than ~300 km may be too cold (24,  
219 29, 39), to explain the hottest Hawaiian basalts (46).

220 LVZs that occur sporadically near 400 and 700 km depth (63, 64) may have similar explanations  
221 (2, 23) and do not require recycling of water and crustal components to the base of the mantle and  
222 back through a water filter [see S12]. Many geochemical and geodynamic models assume whole  
223 mantle convection at the outset, and ignore the effects of dynamic melting and CO<sub>2</sub> when interpreting  
224 LVAs (62, 64).

225

## 226 **Appendix 1 - Dynamic melting**

227 It is now well established that seismic waves can interact with phase changes and that this lowers  
228 seismic wavespeeds (1, 7, 8). Several experimental studies of elastic properties during the melting  
229 process (1, 18, 22, 23) were used in earlier conclusions about the role of melts in the LVZ. One  
230 investigation (1) used a salt-water mixture that produced a binary melting relation (Fig. 2). Two  
231 compositions were studied, 1% and 2% NaCl solutions, that yielded a factor of two difference in the  
232 amounts of melt ( $F$ ) at a given temperature. It was found that at the eutectic temperature of the 1% [2%]  
233 system, the formation of 3% [6%] liquid, was accompanied by a shear modulus drop of about 25%  
234 [60%] and a bulk modulus drop of 8% [30%]. Furthermore, for the same melt content, the bulk modulus  
235 decrease in the low-salt system, relative to the unmelted solid, was about 1/3 and the shear modulus  
236 decrease was 1/2 of that for the high-salt system. In other words, wavespeeds are not simply related to  
237 melt content.

238 Laboratory (1, 7, 8, 18, 21-23) and seismic results (10-12, 14) challenge the standard static two-  
239 phase aggregate models (15) for partial melting in three respects: 1) The shear, longitudinal and bulk  
240 moduli all abruptly decrease at the onset of melting and by more than that due to the geometric effects of  
241 such small melt volumes, 2) The moduli drops are not determined only by the fraction of melt present  
242 and the melt geometry. The dynamic melting model (21) is compatible with these observations since it is  
243 the pressure derivative,  $dF/dP$ , not  $F$ , that dictates the amount of decrease, and 3) The observed velocity  
244 changes for P waves and S waves are comparable, both at the top and the base of the LVZ and the

245 inferred changes in bulk modulus, are significant (8, 21-23). The onset of melting of peridotite (21) is  
246 associated with a relative drop in P velocity that is equal to the relative drop in shear velocity. A seismic  
247 wave interacting with a part of the mantle at its solidus is slowed more than a wave interacting with an  
248 equal amount of melt at higher temperatures (1, 7, 8, 18, 21-23), consistent with dynamic melting, which  
249 depends on  $dF/dP$ . This interaction also explains the large effect on bulk modulus and the anelasticity of  
250 the LVZ. Hence, laboratory studies support the dynamic melting model but are incompatible with inert  
251 two-phase aggregate models (15).

252 While there are a variety of mechanisms that can explain decreasing seismic wavespeeds with depth  
253 (9, 24, 35, 36, 65), the logically dubious argument is sometimes made that since such mechanisms exist,  
254 the partial melt explanation can be ruled out (15). Many of these mechanisms, however, are concerned  
255 only with relaxation of the shear modulus and do not explain the seismic discontinuities at the  
256 boundaries of the LVZ, the strong seismic anisotropy in the LVZ and the laboratory experiments on  
257 dynamic melting that led to the suggestion in the first place (1, 4). At the other extreme, some studies  
258 assume that any LVZ is due to dehydration melting and confirms the presence of large amounts of water  
259 at depth in the mantle.

260 Some arguments against partial melting refer to laboratory studies that claim to observe large  
261 reductions in wavespeeds at subsolidus conditions. However, these studies actually involved melting at  
262 grain boundaries or unaccounted for losses to the apparatus (18, 65). Minimum LVZ wavespeeds have  
263 been overestimated and large subsolidus temperature derivatives for Vs have been used in the arguments  
264 against the need for partial melting in the LVZ (15, 35, 36); low-resolution tomographic models do not  
265 recover the lowest wavespeeds in the boundary layer (13, 56). Tomography, by its nature, averages over  
266 large volumes. Melting in the LVZ of the upper boundary layer appears to be unavoidable, even for the  
267 low ambient temperatures and relatively refractory compositions that have been adopted in laboratory  
268 experiments (16, 21, 46).

269 Two of the most recent arguments that have been used against the presence of melt in the shallow  
270 mantle assume an unsheared homogeneous matrix with no permeability barriers, and extraordinarily  
271 efficient melt extraction mechanisms (15); 1) melts in the mantle do not wet grain boundaries and hence  
272 the ability of partial melt to influence physical properties is limited, and 2) it difficult to retain melt in a  
273 gravity field; gravity will effectively drain out all the melt and gravity-driven fluid dynamic instabilities  
274 will destroy melt-rich layers. The same arguments, if valid, could be used against the water filter model  
275 (62), that assumes that melts accumulate at 410 and 700 km depths.

276 Arguments to the effect that partial melt models for the low velocity zone can be ruled out based on  
277 the wettability of grain boundaries, the aspect ratio of thin film melts and dihedral angles are viewing the  
278 phenomenon at the wrong scale. In a polyphase mélange the melt pockets are sheared into discontinuous  
279 lamellae that have the same effects on long wavelength seismic waves as grain boundary films but which  
280 are independent of wetting angles and surface tension (10, 24).

281

282

### 283 **Appendix 2 - The Transition Zone water filter model and dehydration melting**

284 In addition to the low-velocity zone at the top of the mantle, others have been detected at depths of  
285 roughly 350-370, 400-410 and 600-700 km (46, 62-66). These have been explained by CO<sub>2</sub> and the  
286 accumulation of eclogite, or other crustal components. In the water filter model (62) it is assumed that  
287 broad upwelling currents dehydrate and melt as they pass through the 410-km discontinuity, leaving  
288 water, melt and impurities behind. Lower mantle LVZs are attributed to diffuse downwellings that  
289 dehydrate as they sink below 650 km (64), whole mantle convection being assumed. Transition zone  
290 properties, however, are consistent with cold mantle accumulating above, depressing the 650-km  
291 discontinuity, displacing older warmer mantle upwards, elevating the 410; they are not consistent with  
292 whole mantle convection with throughgoing slabs and hot plumes (19). Alternative explanations of deep  
293 LVAs are CO<sub>2</sub>, segregated basalt, metastability, underplating and interaction of the seismic waves with  
294 phase changes. None of these require whole mantle convection, deep slab penetration or transport of  
295 water into the lower mantle and then back again to 410 km (9, 24).

296 Low-velocity anomalies (LVAs) are often simply attributed to excess temperature or water content,  
297 small grain size or decompression and dehydration melting, but the actual situation is much more  
298 complex and requires mechanisms for causing these phenomena. A horizontal LVZ can be due to the  
299 effects of CO<sub>2</sub>, ponding under a permeability barrier or a negative Clapyron slope boundary, shearing,  
300 metastable phases or the dynamic effects discussed in this paper. Deep LVAs can form at solid-solid  
301 phase boundaries and do not require the presence of either water or of melt (7, 8).

302 The transition-zone water filter and dehydration melting models (62, 64) assume that water is the  
303 main 'impurity' that lowers melting points and that the transition zone is the major water reservoir in the  
304 mantle. Melts and impurities accumulate above and below the transition zone but not in the shallow LVZ  
305 (15). In these models, the global mantle flow pattern is dominated by slab-related localized downwelling  
306 currents and diffuse upwelling flow. This is the precise opposite of the mantle plume model, which

307 assumes narrow focused upwellings (plumes) and diffuse downflow. Alternatively, ancient ambient  
 308 depleted mantle at the base of the TZ is forced up by the downward flux of subducting slabs and  
 309 becomes the passive depleted upwellings that fuel midocean ridges and near-ridge hotspots. Those that  
 310 rise midplate interact with the surface boundary layer and pick up the impurities and chemical  
 311 components that define midplate basalts (24). Volatiles and impurities are sheared into the surface  
 312 boundary layer and this, not the regions above the TZ or the core, is the source of Hawaii, Samoa,  
 313 Yellowstone and other intraplate volcanoes.

314

315 **References**

316

- 317 1. Spetzler HA, Anderson DL (1968) The effect of temperature and partial melting on velocity and  
 318 attenuation in a simple binary system. *J. Geophys. Res.* 73: 6051–6060.
- 319 2. Birch F (1969) in: *The Earth's Crust and Upper Mantle, Geophys. Monograph 13*. (Am. Geophys.  
 320 Union, Washington, DC, pp 18–36.
- 321 3. Birch F (1970) Interpretations of the low velocity zone. *Phy. Earth Planet Int.* 3: 178–181.
- 322 4. Anderson DL, Sammis, CG (1970) Partial melting in the upper mantle. *Phys. Earth Planet. Inter.* 3:  
 323 41–50.
- 324 5. Anderson DL, Spetzler HA (1970) Partial melting and the low-velocity zone. *Phys. Earth Planet.*  
 325 *Inter.* 4: 62–64.
- 326 6. Anderson DL (1970) Petrology of the mantle. *Min. Soc. Am. Spec. Pap.* 3: 85–93.
- 327 7. Vaisnys JR (1968) Propagation of Acoustic Waves through a System Undergoing Phase  
 328 Transformations. *J. Geophys. Res.* 73: 7675–7683.
- 329 8. Li L, Weidner DJ (2008) Effect of phase transitions on compressional-wave velocities in the Earth's  
 330 mantle. *Nature* 454: 984.
- 331 9. Anderson DL (2007) *New Theory of the Earth* (Cambridge Univ. Press, New York).
- 332 10. Kawakatsu H *et al.* (2009) Seismic evidence for sharp lithosphere–asthenosphere boundaries of  
 333 oceanic plates. *Science* 324: 499–502.
- 334 11. Collins J, Vernon F, Orcutt J, Stephen R. (2002) Upper mantle structure beneath the Hawaiian  
 335 swell: constraints from the ocean seismic network pilot experiment. *Geophys. Res. Lett.* 29:  
 336 doi:10.1029/2001GL0133022002.
- 337 12. Gaherty JB, Jordan TH, Gee LS (1996) Seismic structure of the upper mantle in a central Pacific  
 338 corridor. *J. Geophys. Res.* 101: 22291–22309.
- 339 13. Tan Y, Helmberger DV (2007) Trans-Pacific upper mantle shear velocity structure. *J. Geophys. Res.*  
 340 112: doi:10.1029/2006JB004853.
- 341 14. Regan J, Anderson DL (1984) Anisotropic models of the upper mantle. *Phys. Earth and Planet. Int.*  
 342 35: 227–283.
- 343 15. Karato, SI (2013) Does partial melting explain geophysical anomalies? *Physics of the Earth and*  
 344 *Planetary Interiors*: doi:http://dx.doi.org/10.1016/j.pepi.2013.08.006.
- 345 16. Hirschmann MH (2010) Partial melt in the oceanic low velocity zone. *Phy. Earth Planet Int.* 179:  
 346 60–71.
- 347 17. Gribb TT, Cooper RF (2000) The effect of an equilibrated melt phase on the shear creep and  
 348 attenuation behavior of polycrystalline olivine. *Geophys. Res. Lett.* 27: 2173–2352.

- 349 18. Berckhemer H (1980) High-temperature anelasticity and elasticity of mantle peridotite — reply.  
 350 *Phys. Earth Planet. Inter.* 23: 235.
- 351 19. Anderson DL (2013) The persistent mantle plume myth. *Austr. J. of Earth Sci.* 60: 657-673.
- 352 20. Takei Y (2000) Acoustic properties of partially molten media studied on a simple binary system  
 353 with a controllable dihedral angle. *J. Geophys. Res.* 105: 16,665–16,682 doi:10.1029/2000JB  
 354 900124.
- 355 21. Li L, Weidner DJ (2013) Effect of dynamic melting on acoustic velocities in a partially molten  
 356 peridotite. *Phys. Earth Planet. Int.* 222: 1-7.
- 357 22. Mizutani H, Kanamori H (1964) Variation in elastic wave velocity and attenuative property near the  
 358 melting temperature. *J. Phys. Earth* 12: 43-49.
- 359 23. Sato H, Sacks IS, Murase T (1989) The use of laboratory velocity data for estimating temperature  
 360 and partial melt fraction in the low-velocity zone –comparison with heat-flow and electrical-  
 361 conductivity studies, *J. Geophys. Res.* 94: 5689–5704.
- 362 24. Anderson DL (2010) Hawaii, Boundary layers and ambient mantle—geophysical constraints. *J.*  
 363 *Petrology*: doi: 10.1093/petrology/egq068.
- 364 25. Jackson MG *et al.* (2010) Evidence for the survival of the oldest terrestrial mantle reservoir. *Nature*  
 365 466: 853–856 doi:10.1038/Nature09287.
- 366 26. Meibom A, Sleep NH, Zahnle K, Anderson DL (2005) in *Plates, Plumes and Paradigms*, eds.  
 367 Foulger GR, Natland DC, Presnall DC, Anderson DL (Geol. Soc. Amer. Spec. Paper 388), pp.  
 368 347-363.
- 369 27. Huang S, Lee C-TA, Yin Q-Z (2014) Missing lead and high  $^3\text{He}/^4\text{He}$  in ancient sulfides  
 370 associated with continent formation. *Nature Scientific Reports* 4: 5314  
 371 doi:10.1038/srep05314.
- 372 28. Fitton G (2007) The OIB paradox. *GSA Spec. Papers* 430: 387-41.
- 373 29. Moore WB (2008) Heat transport in a convecting layer heated from within and below. *J. Geophys.*  
 374 *Res.* 113: 2156-2202 doi:10.1029/2006JB004778.
- 375 30. Hart SR, Hauri EH, Oschmann LA, Whitehead JA (1992) Mantle plumes and entrainment: isotopic  
 376 evidence. *Science* 256: 517-520 doi:10.1126/science.256.5056.517.
- 377 31. McKenzie D, Bickle MJ (1988) The volume and composition of melt generated by extension of the  
 378 lithosphere. *J. Petrology* 29: 625 – 679.
- 379 32. Humphreys ED, Schmandt B (2003) Looking for mantle plumes. *Phys. Today* 64: 34-39.
- 380 33. DePaolo DJ, Manga M (2003) Deep origin of hotspots – the mantle plume model. *Science* 300: 920-  
 381 921.
- 382 34. Hoffman AW, Hart SR (1978) Assessment of local and regional isotopic equilibrium in the mantle.  
 383 *Earth Planet. Sci. Lett.* 38: 44–62.
- 384 35. Priestley K, McKenzie D (2006) The thermal structure of the lithosphere from shear wave  
 385 velocities. *Earth Planet. Sci. Lett.* 244: 285–301.
- 386 36. Stixrude L, Lithgow-Bertelloni C (2005) Mineralogy and elasticity of the oceanic upper mantle:  
 387 Origin of the low velocity zone. *J. Geophys. Res.* 110: doi:10.1029/2004JB002965.
- 388 37. Schmandt B, Humphreys ED (2010) Complex subduction and small-scale convection revealed by  
 389 body wave tomography of the western U.S. upper mantle. *Earth and Planet. Science Letters*  
 390 297: 435-445, doi:10.1016/j.epsl.2010.06.047.
- 391 38. Hillier JK, Watts AB (2005) Relationship between depth and age in the North Pacific Ocean. *J.*  
 392 *Geophys. Res.* 110: doi:10.1029/2004JB003406.
- 393 39. Jeanloz R, Morris S (1987) Is the mantle geotherm subadiabatic. *Geophys. Res. Lett.* 14: 335–338.

- 394 40. Tackley P, Stevenson D, Glatzmaier G, Schubert G (1993) Effects of an endothermic phase  
 395 transition at 670 km depth in a spherical model of convection in the Earth's mantle. *Nature* 361:  
 396 699–704.
- 397 41. Schuberth BS *et al.* (2009) Thermal versus elastic heterogeneity in high-resolution mantle  
 398 circulation models with pyrolite composition. *Geochem. Geophys. Geosyst.* 10:  
 399 *doi:10.1029/2008GC002235*.
- 400 42. Gale A, Langmuir CH, Dalton CA (2014) The global systematics of ocean ridge basalts and their  
 401 origin. *J. Petrology* 55: 1051-1082 *doi:10.1093/petrology/egu017*.
- 402 43. M. H. Ritzwoller MH, N. M. Shapiro NM, S.-J. Zhong S-J (2004) Cooling history of the Pacific  
 403 lithosphere. *Earth Planet Sci. Lett.* 226: 69–84.
- 404 44. Maggi A, Debayle E, Priestley K, Barroul G (2006) Multimode surface waveform tomography of  
 405 the Pacific Ocean: a closer look at the lithospheric cooling signature. *Geophys. J. Int.* 166: 1384-  
 406 1397.
- 407 45. Haase KM (1996) The relationship between the age of the lithosphere and the composition of  
 408 oceanic magmas. *Earth Planet Sci. Lett.* 144: 75-92.
- 409 46. Presnall DC, Gudfinnsson GH (2011) Oceanic volcanism from the low-velocity zone—geodynamic  
 410 implications. *J. Petrology* 52: 1533-1546.
- 411 47. Wilson JT (1963) A possible origin of the Hawaiian Islands. *Canadian J. Phys.* 41: 863–870.
- 412 48. Van Ark E, Lin J (2004) Time variation in igneous volume flux of the Hawaii-Emperor hot spot  
 413 seamount chain. *J. Geophys. Res.* 109: *doi:10.1029/2003JB002949*.
- 414 49. Hart SR *et al.* (2000) Vailulu’u undersea volcano: The New Samoa. *Geochem. Geophys. Geosyst.* 1:  
 415 Paper number 2000GC00010.
- 416 50. Holtzman BK, Kendall J-M (2010) Organized melt, seismic anisotropy, and plate boundary  
 417 lubrication. *Geochem. Geophys. Geosyst.* 11: *doi:10.1029/2010GC003296*.
- 418 51. Deuss A, Woodhouse JH (2002) A systematic search for mantle discontinuities using SS-precursors.  
 419 *Geophys. Res. Lett.* 29: 90-1 – 90-4 *doi: 10.1029/2002GL014768*.
- 420 52. Hirth G, Kohlstedt DL (1996) Water in the oceanic upper mantle: implications for rheology, melt  
 421 extraction and the evolution of the lithosphere. *Earth Planet. Sci. Lett.* 144: 93–108.
- 422 53. Karato S (2012) On the origin of the asthenosphere. *Earth Planet. Sci. Lett.* 321/322: 95-103.
- 423 54. Holtzman BK *et al.* (2003) Stress-driven melt segregation in partially molten rocks. *Geochem.*  
 424 *Geophys. Geosyst.* 4: *doi:10.1029/2001GC000258*.
- 425 55. Ricard Y, Matas J, Chambat F (2009) Seismic attenuation in a phase change coexistence loop. *Phys.*  
 426 *Earth Planet. Inter.* 176: 124–131.
- 427 56. Styles E *et al.* (2011) Synthetic images of dynamically predicted plumes and comparison with a  
 428 global tomographic model. *Earth Planet. Sci. Lett.* 311: 351–363.
- 429 57. Katzman R, Zhao L, Jordan TH (1998) High-resolution, two-dimensional vertical tomography of the  
 430 central Pacific mantle using ScS reverberations and frequency-dependent travel times. *J.*  
 431 *Geophys. Res.* 103: 17933-17971.
- 432 58. Goes S, Eakin CM, Ritsema J (2013) Lithospheric cooling trends and deviations in oceanic PP-P  
 433 and SS-S differential traveltimes. *J. Geophys. Res.* 118: 996–1007 *doi:10.1002/jgrb.50092*.
- 434 59. Leahy GM *et al.* (2010) Underplating of the Hawaiian Swell: Evidence from teleseismic receiver  
 435 functions. *Geophys. J. Int.* 183: 313-329.
- 436 60. Cañón-Tapia E (2010) Origin of Large Igneous Provinces: The importance of a definition. in  
 437 *Geological Society of America Special Paper* 470, eds Cañón-Tapia E, Szakács A, pp. 77–  
 438 101.
- 439 61. Silver PG *et al.* (2006) Understanding cratonic flood basalts. *Earth Planet. Sci. Lett.* 245: 190–

- 140 201 doi: 10.1016/j.epsl.2006.01.050.
- 141 62. Bercovici D, Karato S (2003), Whole mantle convection and transition-zone water filter. *Nature*
- 142 425: 39-44.
- 143 63. Blum J, Shen Y (2004) Thermal, hydrous, and mechanical states of the mantle transition zone
- 144 beneath southern Africa. *Earth Planet. Sci. Lett.* 217: 367-378.
- 145 64. Schmandt B *et al.* (2014) Dehydration melting at the top of the lower mantle. *Science* 344: 1265-
- 146 1268.
- 147 65. McCarthy C, Takei Y, Hiraga T (2011) Experimental study of attenuation and dispersion over a
- 148 broad frequency range: 2. The universal scaling of polycrystalline materials. *J. Geophys. Res.*
- 149 116: doi:10.1029/2011JB008384.
- 150 66. Keshav S, Gudfinnsson GH, Presnall D (2011) Melting Phase Relations of Simplified Carbonated
- 151 Peridotite at 12-26 GPa in the Systems CaO-MgO-SiO<sub>2</sub>-CO<sub>2</sub> and CaO-MgO-Al<sub>2</sub>O<sub>3</sub>-SiO<sub>2</sub>-CO<sub>2</sub>:
- 152 Highly Calcic Magmas in the Transition Zone of the Earth. *J. Petrology* 52: 2265-2291.

### 153 **Figure Captions**

154 **Figure 1.** Seismic velocities in the LVZ (panel A; modified from refs. 14 and 43) are a function of T

155 and the number-density of melt-rich lamellae. The velocities  $V_{SV}$  of SV waves are mainly controlled

156 by the low-velocity melt-rich or low-rigidity lamellae illustrated schematically in panel B. Decreases

157 in velocities are caused by large positive temperature gradients and partial melting. The SV-SH

158 splitting is caused by melt-rich lamellae shown schematically in panel C, which are sheared by plate

159 motion as indicated by the arrow. The strong increase in velocities below about 150 km, which has

160 been considered enigmatic (36), is due to subadiabatic or negative temperature gradients (39-41)

161 (panel B).

162 **Figure 2.** Decreases in longitudinal and shear velocities across the solidus in dilute (1% and 2%)

163 NaCl-H<sub>2</sub>O solutions (*I*). The temperatures are scaled to the eutectic temperature ( $T^* = -21.1$  C) as  $(T -$

164  $T^*)/|T^*|$ . The velocities  $V_L$  and  $V_S$  are scaled to  $V_0$ , the corresponding values in pure ice at the

165 lowest measured temperature  $(T - T^*)/|T^*| = -0.6$ . The percent of liquid melt relative to solid ice is also

166 indicated. This provides an analog to the G discontinuity that separates the high wavespeed seismic

167 lid from the low velocity zone (LVZ). The theory that explains these laboratory results has been

168 confirmed at seismic frequencies (21). The effects of aligned melt-rich lamellae and dynamic melting

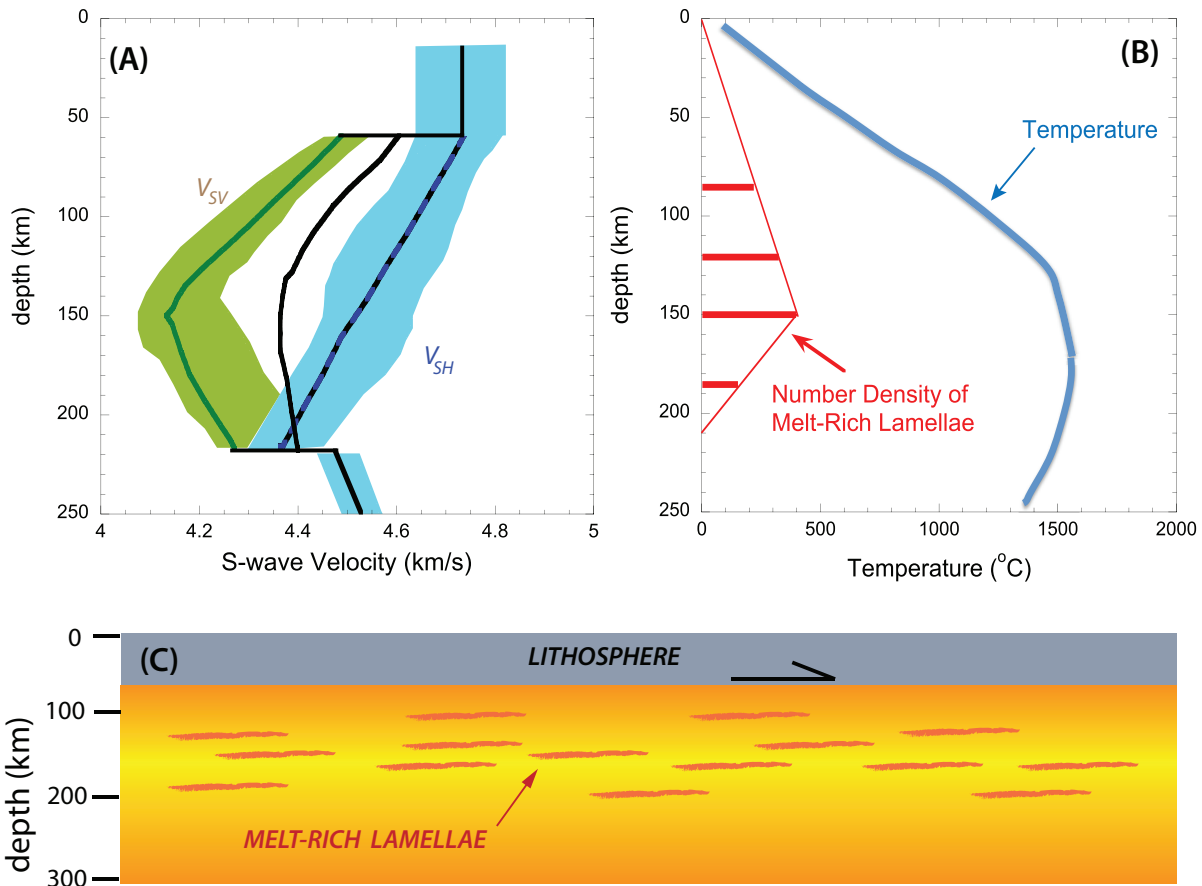
169 accentuate the effects of small degrees of melt, particularly on the longitudinal and bulk moduli. In

170 addition, melt migration may increase the amount of melt relative to equilibrium partial melting

171 calculations (16).

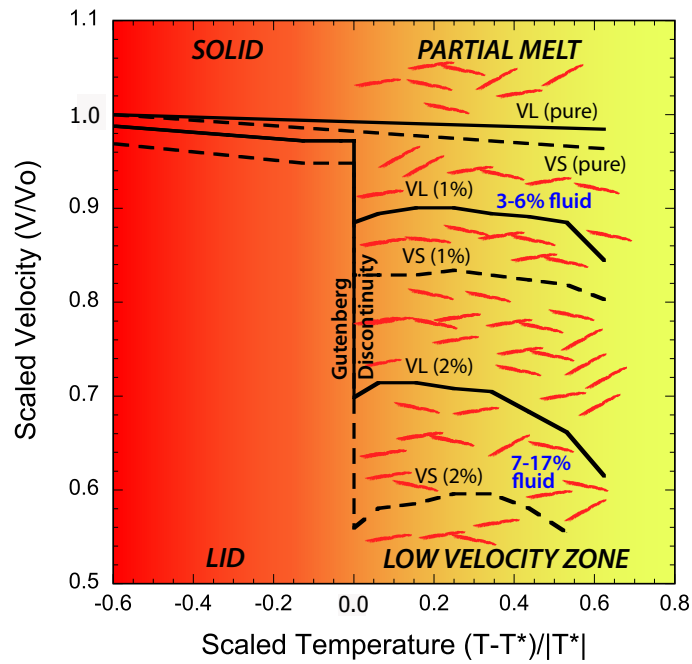
172

476  
477



478  
479

FIG 1



480  
481

FIG 2